Dynamical structure of paramagnetic $[M(H_2O)_6][SiF_6]$ ($M = Fe^{2+}, Ni^{2+}$) crystal studied by means of $^2H$ nuclear magnetic resonance



2000 J. Phys.: Condens. Matter 12 7261

(http://iopscience.iop.org/0953-8984/12/32/310)

J. Phys.: Condens. Matter **12** (2000) 7261–7273. Printed in the UK PII: S0953-8984(00)13403-4

# Dynamical structure of paramagnetic $[M(H_2O)_6][SiF_6]$ ($M = Fe^{2+}, Ni^{2+}$) crystal studied by means of $^2H$ nuclear magnetic resonance

M Mizuno†, T Iijima and M Suhara

Department of Chemistry, Faculty of Science, Kanazawa University, Kanazawa 920-1192, Japan

E-mail: mizuno@wriron1.s.kanazawa-u.ac.jp

Received 19 April 2000, in final form 30 June 2000

**Abstract.** The temperature dependences of the $^2H$ nuclear magnetic resonance (NMR) spectra and the spin–lattice relaxation time $T_1$ were measured for $[Ni(H_2O)_6][SiF_6]$ and $[Fe(H_2O)_6][SiF_6]$. The motional modes for both compounds were discussed on the basis of the spectral simulation. The temperature variations of the $^2H$ NMR spectra at high temperatures could be explained by three-site jumps of $[Ni(H_2O)_6]^{2+}$ about the $C_3$ axis for $[Ni(H_2O)_6][SiF_6]$. For $[Fe(H_2O)_6][SiF_6]$, however, six-site jumps of $[Fe(H_2O)_6]^{2+}$ about the $C_3$ axis were found to be most probable form of motion at high temperatures. At low temperatures, the $^2H$ NMR spectra of both compounds could be explained by 180° flips of the water molecule. The $^2H$ NMR $T_1$ was dominated by the fluctuations of the electric field gradient caused by the molecular motion and of the magnetic interaction between the $^2H$ nucleus and the unpaired electron spin in the metal ion. $T_1$ was analysed in terms of the motional modes predicted from the spectral simulation. The activation energies, the jumping rates at infinite temperature for each form of motion and the quadrupole interaction parameters ($e^2Qq/h, \eta$) were obtained from the $^2H$ NMR spectra and $T_1$. The conclusions from the spectral simulation are in good agreement with the results for $T_1$. These results suggest that $[Fe(H_2O)_6][SiF_6]$ possesses dynamic disorder structure in the high-temperature phase.

## 1. Introduction

A number of studies on the phase transition and the disorder structure of $[M(H_2O)_6][SiF_6]$ ($M = Mg, Mn, Fe, Co, Ni, Zn$) crystal have been performed [1–12]. These compounds have similar crystal structures and form a rhombohedrally distorted CsCl-type structure. The $[M(H_2O)_6]^{2+}$ and $[SiF_6]^{2-}$ octahedra are stacked in columns parallel to the $\bar{3}$ axis. For the symmetry of the original phase, these compounds are divided into two classes. Those with M = Co, Ni and Zn are in the same class [3–5]. The space group of this class is $R\bar{3}$ and there is disorder of the $[SiF_6]^{2-}$ octahedron around the $C_3$ axis. For M = Ni, the disordered $[SiF_6]^{2-}$ octahedra are related by 30° rotation around the $C_3$ axis, whereas there is no disorder of $[Ni(H_2O)_6]^{2+}$ [3]. The quadrupole coupling tensors and the jumping rates of the $[Ni(H_2O)_6]^{2+}$ ion and the water molecule for M = Ni have been determined by single-crystal $^2H$ NMR measurements [13]. Compounds with M = Mg, Fe and Mn are in another class and have the space groups $R\bar{3}m$, $R\bar{3}m$ and $P\bar{3}m1$, respectively [1, 2, 6, 7]. The disordered $[M(H_2O)_6]^{2+}$ and $[SiF_6]^{2-}$ octahedra exist randomly in two different orientations related by the mirrors containing the threefold axis. For M = Mg, Mn, Fe and Co, the compounds exhibit phase

† Author to whom any correspondence should be addressed.

0953-8984/00/327261+13$30.00  

transition. The M = Fe compound undergoes a phase transition at $T_c = 240$ K and the space group becomes $P2_1/c$ in the low-temperature phase [2]. In the high-temperature phase, two different orientations of the disordered $[Fe(H_2O)_6]^{2+}$ and $[SiF_6]^{2-}$ octahedra are related by 18° and 54° rotation around the $C_3$ axis, respectively [1]. The previous investigation using the $^1H$ and $^{19}F$ NMR $T_1$ has shown a change in the crystal field of $[Fe(H_2O)_6]^{2+}$ due to the phase transition [10]. However, information on the molecular motion was not obtained.

Recently, we have studied the molecular motions in the M = Mg and Co compounds by measuring the $^2H$ NMR spectrum and the spin–lattice relaxation time $T_1$ [11, 12]. From these studies, it was confirmed that three-site jumps about the $C_3$ axis occur most frequently for the $[M(H_2O)_6]^{2+}$ ion of both compounds at high temperatures and this form of motion is closely related to the phase transition.

In the present work, we investigated the phase transition and the disorder structure of the M = Fe compound from the dynamic viewpoint by analysing the $^2H$ NMR spectrum and $T_1$ for the powder sample. Moreover, the electron spin dynamics of $Fe^{2+}$ was studied. The thermal anomalies of the deuterated and protonated M = Fe compound were also examined by differential thermal analysis (DTA). The $^2H$ NMR spectrum and $T_1$ for the M = Ni compound, which does not undergo a phase transition, were measured for comparison. The $^2H$ NMR spectral simulation was performed by considering the quadrupole interaction and the dipole interaction between the $^2H$ nucleus and the metal ion [12, 14–19]. $T_1$ was analysed by calculating the correlation function for each form of motion [20]. Since the $^2H$ NMR spectrum is sensitive to the motional mode of the molecule and the ion, it is considered to be easy to distinguish between three-site and six-site jumps and to clarify whether the disorder of $[Fe(H_2O)_6]^{2+}$ is dynamic or static.

## 2. Experimental procedure

The deuterated samples were obtained by repeated recrystallization from heavy water. The $^2H$ NMR spectra were measured by using a CMX-300 spectrometer at 45.825 MHz. A shift-compensated pulse sequence, $(\pi/2)_x$–$\tau/2$–$(\pi)_y$–$\tau/2$–$(\pi/2)_y$–$\tau/2$–$(\pi)_y$–$\tau/2$–acq, was used [12, 14–17], which refocuses the dephasing due to the quadrupole interaction and the paramagnetic shift. The $\pi/2$ pulse width and $\tau/2$ were 2.0 and 20 $\mu$s, respectively. $T_1$ was measured by the inversion–recovery method. The DTA was performed with a home-made apparatus.

## 3. Results and discussion

### *3.1. DTA*

DTA measurements were performed between 100 and 300 K. For those for deuterated $[Fe(H_2O)_6][SiF_6]$, the heat anomaly due to the phase transition was detected at 229 K on heating and 227 K on cooling. The heat anomaly of protonated $[Fe(H_2O)_6][SiF_6]$ was observed at 224 K on heating and 222 K on cooling. The transition temperature was found to shift to the higher side by 5 K on deuteration.

### *3.2. $^2H$ NMR spectra*

*3.2.1. $[Ni(H_2O)_6][SiF_6]$.* Figure 1(a) shows the $^2H$ NMR spectra of $[Ni(H_2O)_6][SiF_6]$ observed at high temperatures. The spectrum showed the asymmetric line shape due to the paramagnetic shift caused by the dipole interaction between the $^2H$ nuclei and the $Ni^{2+}$ ions.

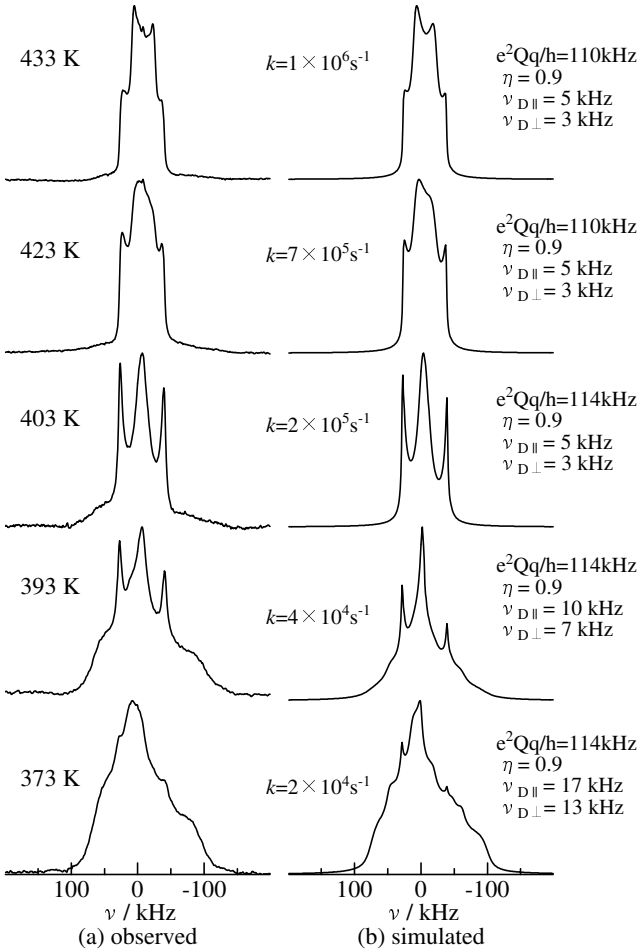


**Figure 1.** The temperature dependence of the $^2$H NMR spectrum of $[Ni(H_2O)_6][SiF_6]$ at high temperatures. (a) and (b) show the observed and the theoretical spectra, respectively. The theoretical spectra were simulated by assuming three-site jumping around the $C_3$ axis.

The change of the line shape can be explained by three-site jumps of $[Ni(H_2O)_6]^{2+}$ about the $C_3$ axis as shown in figure 2(a). The spectral simulation was performed by considering the quadrupole interaction and the dipole interaction between $^2$H nuclei and the $Ni^{2+}$ ions. The site frequency of the $^2$H nucleus is written as [12, 14, 16, 17]

$$\omega_i = \mp\omega_Q - \omega_P. \tag{1}$$

Here, $\omega_Q$ and $\omega_P$ are the contributions of the quadrupole interaction and the dipolar interaction between the $^2$H nuclei and $M^{2+}$ ions and are written in terms of the second-order Wigner rotation matrix as [12, 14, 17, 18, 21]

$$\omega_Q = \sqrt{\frac{3}{2}} \sum_{n,m=-2}^{2} D_{0n}^{(2)*}(\psi, \theta, \phi) D_{nm}^{(2)*}(\alpha, \beta, \gamma) T_{mQ}^{(2)} \tag{2}$$

$$\omega_P = \sum_{n=-2}^{2} D_{0n}^{(2)*}(\psi, \theta, \phi) D_{n0}^{(2)*}(\alpha', \beta', \gamma') \omega_D \tag{3}$$

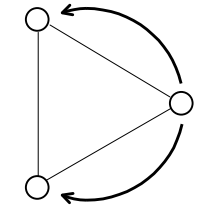

(a) three-site jump

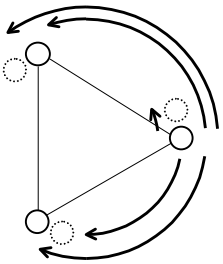

(b) six-site jump

**Figure 2.** $N$-site jumping of $[M(H_2O)_6]^{2+}$ around the $C_3$ axis in $[M(H_2O)_6][SiF_6]$. The circles indicate the water molecules on the top face of the $[M(H_2O)_6]^{2+}$ octahedron. The broken circles indicate the alternative sites according to the disorder structure. Arrows show the possible jumps from a site. (a) shows a three-site jump of $[Ni(H_2O)_6]^{2+}$. (b) shows a six-site jump of $[Fe(H_2O)_6]^{2+}$.

$$T_{0Q}^{(2)} = \sqrt{\frac{3}{8}} e^2 Qq/\hbar \qquad T_{\pm 2Q}^{(2)} = (\eta/4) e^2 Qq/\hbar \tag{4}$$

$$\omega_D = 2\pi \nu_D \tag{5}$$

$$\nu_D = \nu_{Diso} + \frac{1}{2}\left[\nu_{Dzz}(3\cos^2\beta'' - 1) + (\nu_{Dxx} - \nu_{Dyy})\sin^2\beta''\cos 2\gamma''\right] \tag{6}$$

where $(\alpha, \beta, \gamma)$, $(\psi, \theta, \phi)$ and $(\alpha', \beta', \gamma')$ represent the Euler angles for the transformation from the molecular axes to the principal-axis system of the quadrupolar tensor, from the laboratory axes to the molecular axes and from the molecular axes to the principal-axis system of the dipolar tensor between the $^2H$ nuclei and the $M^{2+}$ ion, respectively. $\beta''$ and $\gamma''$ are angles connecting the direction of the external field and the principal-axis system of the $g$-tensor.

In this temperature range, the electric field gradient (EFG) at the $^2H$ nucleus is averaged by the fast 180° flips of the water molecule. The principal-axis system of the averaged EFG tensor $(x_p, y_p, z_p)$ was assigned as follows [22]: the $z_p$-axis is perpendicular to the water molecular plane, the $y_p$-axis lies in the water molecular plane and the $x_p$-axis is parallel to the bisector of D–O–D. $\beta$ and $\gamma$ were estimated as −82.6° and 40.8° from the results of the single-crystal $^2H$ NMR measurements [13], respectively. $\beta'$ was assumed as 53°. $\beta''$ and $\gamma''$ are equal to $\theta$ and $\phi$, since the $g$-tensor is axially symmetric and its $z$-axis is parallel to the threefold axis. The frequencies of the three sites were specified by $(\alpha, \alpha') = (0°, 90°)$, $(120°, 210°)$ and $(240°, 330°)$. Figure 1(b) shows the $^2H$ NMR spectral simulation. Figure 3(a) shows the $^2H$ NMR spectra at low temperatures. The temperature variation of the spectrum is considered to be caused by 180° flips of the water molecule in these temperature ranges. The spectral simulation was performed using the two-site jump model. The molecular axes were specified as the $z$-axis coinciding with the threefold axis and, therefore, $\beta''$ and $\gamma''$ are equal to $\theta$ and $\phi$.

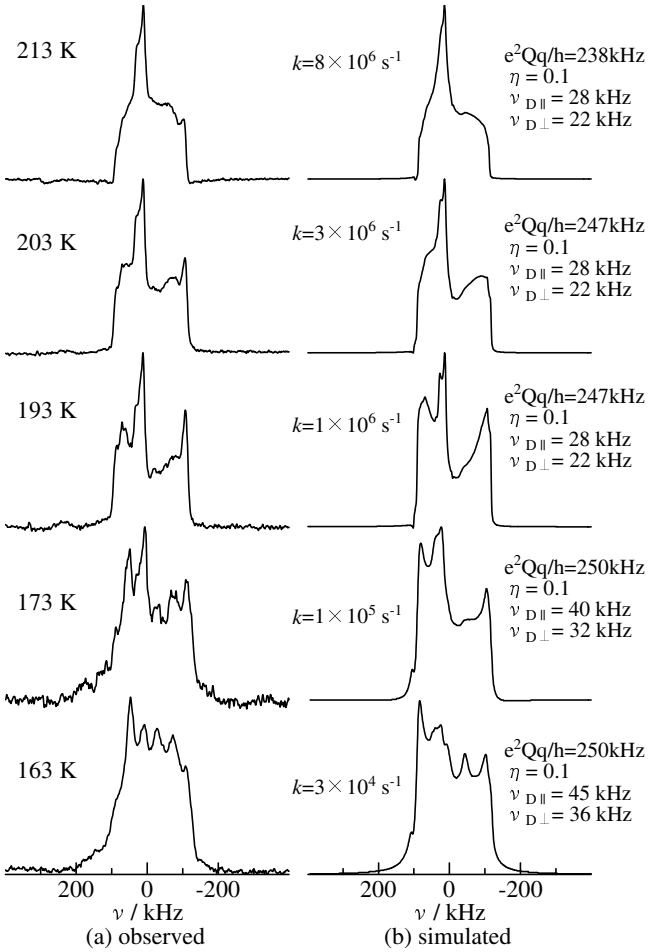


**Figure 3.** The temperature dependence of the $^2H$ NMR spectrum of $[Ni(H_2O)_6][SiF_6]$ at low temperatures. (a) and (b) show the observed and the theoretical spectra, respectively. The theoretical spectra were simulated by assuming two-site jumping of the water molecules.

Two sites of the $^2H$ nucleus of the water molecule were specified by $(\alpha, \beta, \gamma)$ and $(\alpha', \beta', \gamma')$: $(77^\circ, 163^\circ, 32^\circ)$ and $(60^\circ, 20^\circ, 0^\circ)$ for one site; $(53^\circ, 94^\circ, 191^\circ)$ and $(60^\circ, 50^\circ, 0^\circ)$ for the other. The result of the spectral simulation is shown in figure 3(b).

*3.2.2. $[Fe(H_2O)_6][SiF_6]$.* Figure 4(a) shows the $^2H$ NMR spectra of $[Fe(H_2O)_6][SiF_6]$ above $T_c$. The temperatures at which $[Fe(H_2O)_6][SiF_6]$ exhibited a variation of the spectrum were lower than those at which $[Ni(H_2O)_6][SiF_6]$ showed a variation. The intensity of the central portion of the spectra for $[Fe(H_2O)_6][SiF_6]$ decreased with decreasing temperature and a doublet-type feature appeared at 283 K, whereas a strong peak appeared in the centre of the spectrum for $[Ni(H_2O)_6][SiF_6]$. The $^2H$ NMR spectrum of $[Fe(H_2O)_6][SiF_6]$ is considered to be dominated by the quadrupole interaction and the dipole interaction between the $^2H$ nuclei and the metal ions, in analogy with that of $[Ni(H_2O)_6][SiF_6]$. However, these temperature variations of the spectrum for $[Fe(H_2O)_6][SiF_6]$ could not be explained by three-site jumps of $[Fe(H_2O)_6]^{2+}$ about the $C_3$ axis. Another possible motion of $[Fe(H_2O)_6]^{2+}$ at high temperatures

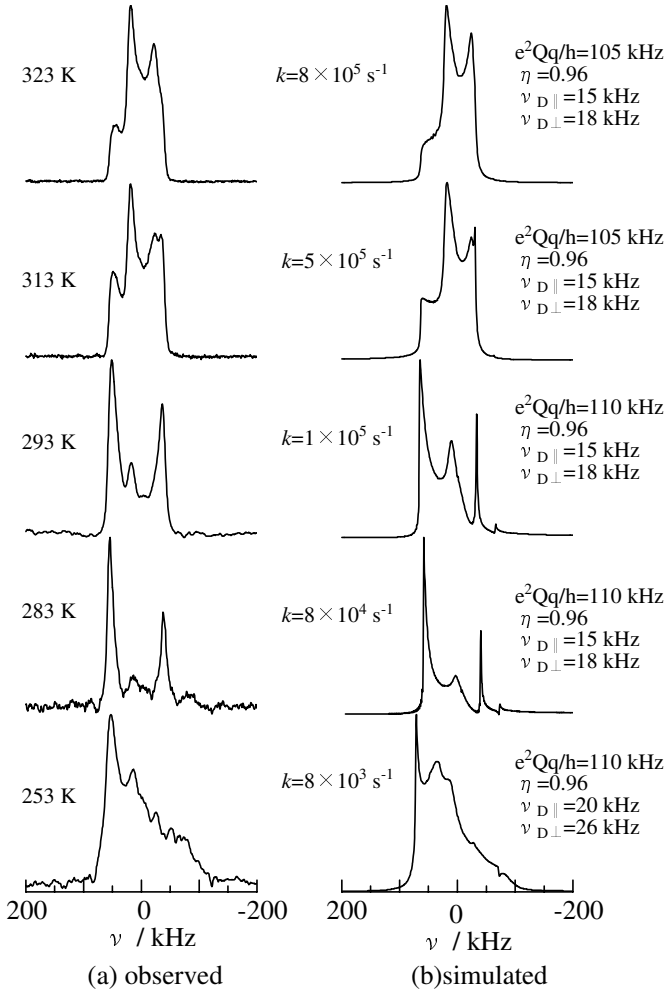


**Figure 4.** The temperature dependence of the $^2$H NMR spectrum of $[Fe(H_2O)_6][SiF_6]$ above $T_c$. (a) and (b) show the observed and the theoretical spectra, respectively. The theoretical spectra were simulated by assuming six-site jumping around the $C_3$ axis.

is six-site jumping about the $C_3$ axis as shown in figure 2(b), since two different orientations of the $[Fe(H_2O)_6]^{2+}$ octahedra and six equivalent sites of the water molecule exist around the $C_3$ axis [1, 2]. This motion gives the decrease of the central portion in the $^2$H NMR spectrum [17]. Figure 4(b) shows the $^2$H NMR spectral simulation performed by assuming the jumps to occur between the six sites with equal probability. The principal-axis system of the EFG tensor which is averaged by the fast 180° flips was assigned in a similar manner to that for $[Ni(H_2O)_6][SiF_6]$. $\beta = -88.8°$ and $\gamma = 50.0°$ were estimated from the results of neutron diffraction analysis [1]. $\beta'$ was assumed as 35.0°. $\beta''$and $\alpha''$ are equal to $\theta$ and $\phi$, respectively. Two orientations of the disordered $[Fe(H_2O)_6]^{2+}$ are related by the 18° rotation about the $C_3$ axis [1]. Therefore, the frequencies of the six sites were specified by $(\alpha, \alpha') = (0°, 82.7°)$, (18°, 100.7°), (120°, 202.7°), (138°, 220.7°), (240°, 322.7°) and (258°, 340.7°). Figure 5(a) shows the $^2$H NMR spectra below $T_c$. The temperature variation of the spectrum is considered to be caused by 180° flips of the water molecule in these temperature ranges. The spectral

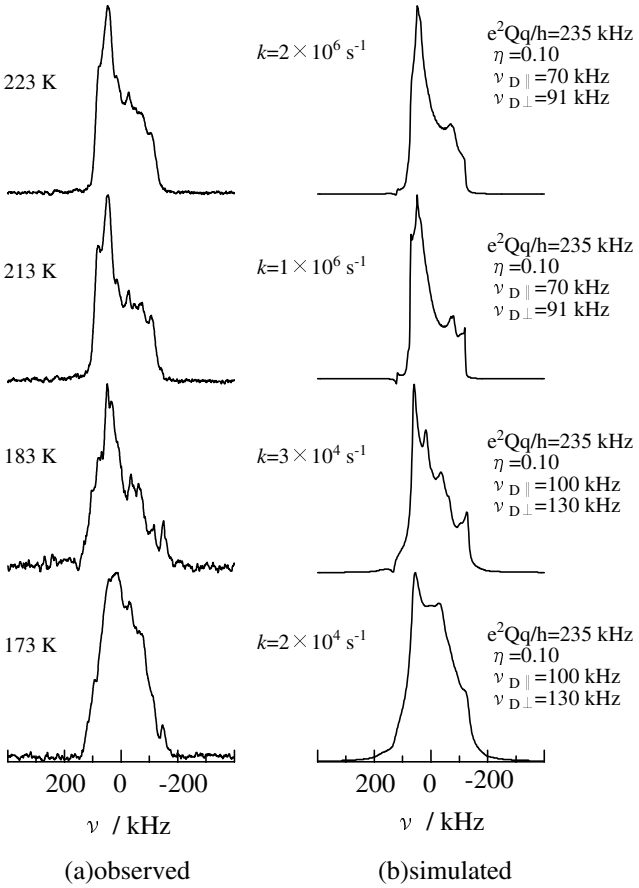


**Figure 5.** The temperature dependence of the $^2$H NMR spectrum of $[Fe(H_2O)_6][SiF_6]$ below $T_c$. (a) and (b) show the observed and the theoretical spectra, respectively. The theoretical spectra were simulated by assuming two-site jumping of the water molecules.

simulation was performed using the two-site jump model. Two sites of the $^2$H nucleus of the water molecule were specified by $(\alpha, \beta, \gamma)$ and $(\alpha', \beta', \gamma')$: $(0^\circ, 5.5^\circ, 0^\circ)$ and $(176^\circ, -38^\circ, 0^\circ)$ for one site; $(168^\circ, -106^\circ, 0^\circ)$ and $(174^\circ, 80^\circ, 0^\circ)$ for the other. The result of the spectral simulation is shown in figure 5(b).

### *3.3. The $^2H$ NMR $T_1$*

*3.3.1. $[Ni(H_2O)_6][SiF_6]$.* Figure 6 shows the temperature dependence of the $^2$H NMR $T_1$ for $[Ni(H_2O)_6][SiF_6]$. The relaxation of $^2$H is considered to be dominated by the fluctuation of the EFG due to $180^\circ$ flips of the water molecule and the magnetic interaction between the $^2$H nuclei and $Ni^{2+}$ ions. The relaxation rate due to $180^\circ$ flips of the water molecule is written as

$$T_{1H_2O}^{-1} = A_{H_2O}\left\{\frac{k}{(2k)^2+\omega_0^2} + \frac{4k}{(2k)^2+4\omega_0^2}\right\} \tag{7}$$

where $\omega_0$ is the angular NMR frequency of the $^2$H nucleus. The jumping rate $k$ is denoted by an Arrhenius relation as

$$k = k_0 \exp(-E_a/RT). \tag{8}$$

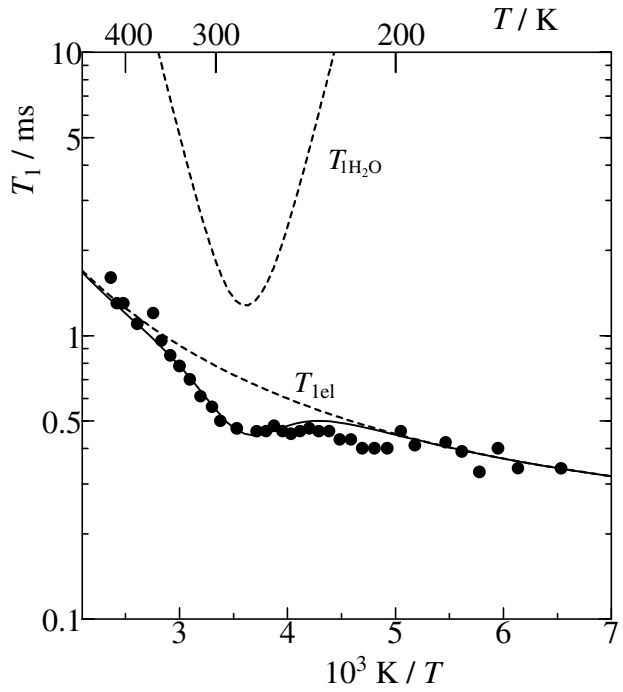


**Figure 6.** The temperature dependence of the $^2$H NMR $T_1$ for $[Ni(H_2O)_6][SiF_6]$. The solid line shows the theoretical fitting curve. The broken lines show the contributions to the relaxation rate.

The contribution of the paramagnetic interaction to $T_1$ is written as [12 ,14, 23]

$$T_{1el}^{-1} = \frac{2}{5}\gamma^2 g^2 \mu_B^2 \sum_i r_i^{-6} S(S+1)\tau_e. \tag{9}$$

Here, $r_i$ is the distance between the $^2$H nucleus and the $i$th $Ni^{2+}$ ion. $\sum_i r_i^{-6}$ was calculated by using the crystal data for $[Ni(H_2O)_6][SiF_6]$ [3]. The electron spin-correlation time $\tau_e$ is given by the temperature-dependent electron spin–lattice relaxation time $T_{1e}$ and the temperature-independent characteristic time for the spin flip due to the electron–electron interaction $\tau_s$ as [23]

$$\tau_e^{-1} = T_{1e}^{-1} + {\tau_s}^{-1}. \tag{10}$$

$T_{1e}$ for $Ni^{2+}$ in $[Ni(H_2O)_6][SiF_6]$ is considered to be dominated by the Raman process at high temperatures and written as [23, 24]

$$T_{1e} = aT^{-2}. \tag{11}$$

The temperature dependence of $T_1$ can be represented by

$$T_1^{-1} = T_{1H_2O}^{-1} + T_{1el}^{-1}. \tag{12}$$

A least-squares fitting calculation was performed using equations (7)–(12) with $A_{H_2O}$, $k_0$, $a$, $E_a$ and $\tau_s$ as parameters. The parameters obtained are listed in table 1.

*3.3.2. [Fe(H$_2$O)$_6$][SiF$_6$].* Figure 7 shows the temperature dependence of the $^2$H NMR $T_1$ for $[Fe(H_2O)_6][SiF_6]$. Below $T_c$, $T_1$ is considered to be dominated by the dipole interaction

**Table 1.** The parameters obtained from the $^2$H NMR spectral simulation and from $T_1$ for $[Ni(H_2O)_6][SiF_6]$.

| | | | |
|---|---|---|---|
| Reorientation of $[Ni(H_2O)_6]^{2+}$ | Spectral simulation | $E_a^{re}$/kJ mol$^{-1}$ | 95 |
| | | $k_{re0}$/s$^{-1}$ | $3.0 \times 10^{17}$ |
| 180° flips of $H_2O$ | Spectral simulation | $A_{H_2O}$/s$^{-2}$ | $2.3 \times 10^{11}$ |
| | | $E_a$/kJ mol$^{-1}$ | 30 |
| | | $k_0$/s$^{-1}$ | $1.7 \times 10^{14}$ |
| | $T_1$ | $A_{H_2O}$/s$^{-2}$ | $3.2 \times 10^{11}$ |
| | | $E_a$/kJ mol$^{-1}$ | 29 |
| | | $k_0$/s$^{-1}$ | $8.8 \times 10^{13}$ |
| Electron spin in $Ni^{2+}$ | $T_1$ | $a$/s K$^2$ | $8.7 \times 10^{-6}$ |
| | | $\tau_s$/s | $3.4 \times 10^{-10}$ |

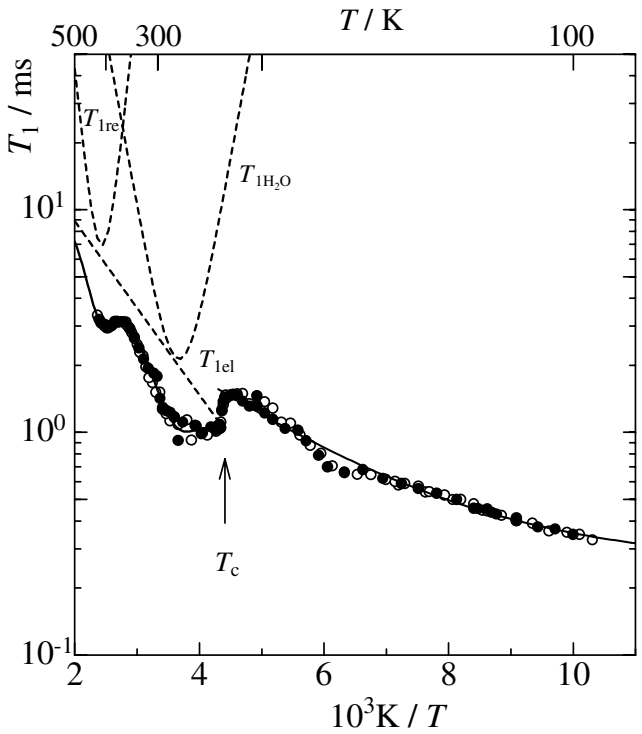


**Figure 7.** The temperature dependence of the $^2$H NMR $T_1$ for $[Fe(H_2O)_6][SiF_6]$. ○ and ● indicate $T_1$ on heating and cooling, respectively. The solid line shows the theoretical fitting curve. The broken lines show the contributions to the relaxation rate.

between the $^2$H nucleus and the $Fe^{2+}$ ion, which is given by equations (9) and (10). $T_{1e}$ for $Fe^{2+}$ in $[Fe(H_2O)_6][SiF_6]$ is considered to be determined by the Orbach process [10] and written as

$$T_{1e} = \tau_{e0} \exp(\Delta / kT) \tag{13}$$

where $\tau_{e0}$ and $\Delta$ are the pre-exponential factor and the energy difference between the ground and excited states that participate in the relaxation of the electron spin, respectively. $\sum_i r_i^{-6}$ was calculated by using the crystal data for $[Fe(H_2O)_6][SiF_6]$ [1]. For the temperature dependence

of $T_1$ below $T_c$, a least-squares-fitting calculation was performed using equations (9), (10) and (13) with $\tau_{e0}$, $\Delta$ and $\tau_s$ as parameters. The parameters obtained are listed in table 2. The minima of $T_1$ observed at ≈400 and 270 K are considered to be due to the reorientation of $[Fe(H_2O)_6]^{2+}$ around the $C_3$ axis and 180° flips of the water molecule, respectively. By assuming the reorientation of $[Fe(H_2O)_6]^{2+}$ between all six equivalent sites around the $C_3$ axis, the relaxation rate $T_{1re}^{-1}$ is written as

$$T_{1re}^{-1} = A_{re}\left\{\frac{k_{re}}{(6k_{re})^2+\omega_0^2}+\frac{4k_{re}}{(6k_{re})^2+4\omega_0^2}\right\} \tag{14}$$

$$k_{re} = k_{re0}\exp(-E_a^{re}/RT). \tag{15}$$

The contribution from 180° flips of the water molecule to the relaxation rate is given by equation (7). The relaxation rate $T_{1el}^{-1}$ due to the dipole interaction between the $^2H$ nucleus and the electron spin of $Fe^{2+}$ is obtained from equations (9) and (13), since the relation $\tau_e \approx T_{1e}$ holds above $T_c$. The temperature dependence of $T_1$ above $T_c$ can be explained by

$$T_1^{-1} = T_{1re}^{-1} + T_{1H_2O}^{-1} + T_{1el}^{-1}. \tag{16}$$

The result of a least-squares fitting performed above $T_c$ using equations (7)–(9) and (13)–(16) with $A_{re}$, $k_{re0}$, $E_a^{re}$, $A_{H_2O}$, $k_0$, $E_a$, $\tau_{e0}$ and $\Delta$ as parameters is shown in figure 7. The parameters obtained are listed in table 2.

**Table 2.** The parameters obtained from the $^2H$ NMR spectral simulation and from $T_1$ for $[Fe(H_2O)_6][SiF_6]$.

| | | | | |
|---|---|---|---|---|
| Reorientation of $[Fe(H_2O)_6]^{2+}$ | Spectral simulation | $T > T_c$ | $A_{re}/s^{-2}$ | $1.9 \times 10^{11}$ |
| | | | $E_a^{re}$/kJ mol$^{-1}$ | 45 |
| | | | $k_{re0}/s^{-1}$ | $1.3 \times 10^{13}$ |
| | $T_1$ | $T > T_c$ | $A_{re}/s^{-2}$ | $1.7 \times 10^{11}$ |
| | | | $E_a^{re}$/kJ mol$^{-1}$ | 50 |
| | | | $k_{re0}/s^{-1}$ | $1.6 \times 10^{14}$ |
| 180° flips of $H_2O$ | Spectral simulation | $T < T_c$ | $A_{H_2O}/s^{-2}$ | $1.9 \times 10^{11}$ |
| | | | $E_a$/kJ mol$^{-1}$ | 33 |
| | | | $k_0/s^{-1}$ | $1.1 \times 10^{14}$ |
| | $T_1$ | $T > T_c$ | $A_{H_2O}/s^{-2}$ | $1.9 \times 10^{11}$ |
| | | | $E_a$/kJ mol$^{-1}$ | 29 |
| | | | $k_0/s^{-1}$ | $8.3 \times 10^{13}$ |
| Electron spin in $Fe^{2+}$ | $T_1$ | $T > T_c$ | $\Delta/cm^{-1}$ | 630 |
| | | | $\tau_{e0}$/s | $1.6 \times 10^{-13}$ |
| | | $T < T_c$ | $\Delta/cm^{-1}$ | 330 |
| | | | $\tau_{e0}$/s | $2.0 \times 10^{-12}$ |
| | | | $\tau_s$/s | $8.5 \times 10^{-11}$ |

### *3.4. Molecular motion and crystal structure*

Figure 8 shows the temperature dependences of the rates for the three-site jumping of $[Ni(H_2O)_6]^{2+}$ about the $C_3$ axis and 180° flips of the water molecule obtained by the spectral simulation. By assuming an Arrhenius relation, the activation energies and the jumping rates at infinite temperature were estimated for these types of motion. The $A_{H_2O}$-value of equation (7)

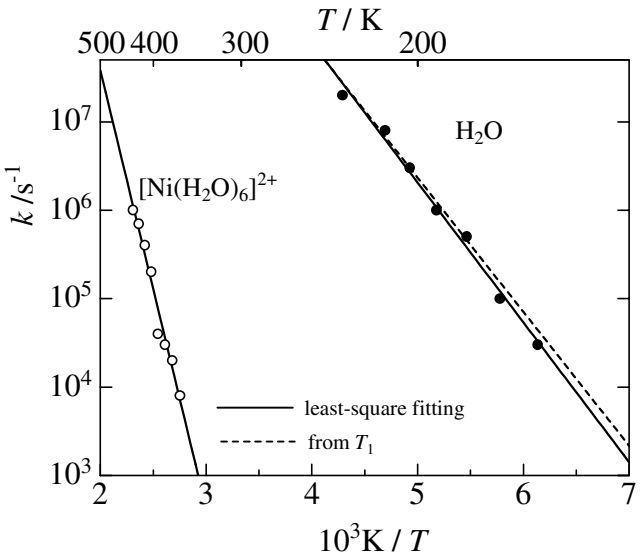


**Figure 8.** Temperature dependences of the jumping rates $k$ for the reorientation of $[Ni(H_2O)_6]^{2+}$ (○) and 180° flips of the water molecule (●) in $[Ni(H_2O)_6][SiF_6]$. The solid lines show the results of the least-squares fitting. The broken line shows the result obtained from $T_1$.

was estimated using $e^2Qq/h$, $\eta$, $\alpha$, $\beta$ and $\gamma$ employed for the spectral simulation by calculating the correlation function [20]. The parameters obtained are listed in table 1.

The full circles in figure 9 show the temperature dependence of $k$ for 180° flips of the water molecule in $[Fe(H_2O)_6][SiF_6]$ obtained by the spectral simulation. The values of $k_0$ and $E_a$ for 180° flips of the water molecule below $T_c$ were obtained by a least-squares fitting as $1 \times 10^{14}$ s$^{-1}$ and 33 kJ mol$^{-1}$, respectively. From $T_1$, $k_0$ and $E_a$ for 180° flips of the water molecule above $T_c$ were estimated as $8.3 \times 10^{13}$ s$^{-1}$ and 29 kJ mol$^{-1}$, respectively. The open circles in figure 9 show the temperature dependence of $k_{re}$ for six-site jumping of $[Fe(H_2O)_6]^{2+}$ about the $C_3$ axis. The solid line shows a least-squares fitting to $k_{re}$ obtained by the spectral simulation. $k_{re0} = 1 \times 10^{13}$ s$^{-1}$ and $E_a^{re} = 45$ kJ mol$^{-1}$ were estimated by the fitting. The temperature dependence of $k_{re}$ obtained from $T_1$, which is shown by the broken line in figure 9, was compatible with that given by the spectral simulation. We estimated the $A_{re}$-value of equation (14) as $1.9 \times 10^{11}$ s$^{-2}$ using $e^2Qq/h$, $\eta$, $\alpha$, $\beta$ and $\gamma$ employed for the spectral simulation by calculating the correlation function [20]. This value is consistent with $A_{re} = 1.7 \times 10^{11}$ s$^{-2}$ obtained from $T_1$. The good agreement between the results of the spectral simulation and those obtained from $T_1$ suggests that the dynamically disordered structure is formed due to six-site jumping of $[Fe(H_2O)_6]^{2+}$ about the $C_3$ axis in the high-temperature phase. The $\Delta$ value of $Fe^{2+}$ was obtained as 630 and 330 cm$^{-1}$ above and below $T_c$, respectively. This decrease of $\Delta$ is considered to be caused by a change in the crystal field of $[Fe(H_2O)_6]^{2+}$ due to the phase transition. The jumping rate for the reorientation of $[Fe(H_2O)_6]^{2+}$ decreases to of the order of $10^3$ s$^{-1}$ at $T_c$. Therefore, a change in the crystal field of $[Fe(H_2O)_6]^{2+}$ is considered to arise from the freezing of the reorientation of $[Fe(H_2O)_6]^{2+}$. The activation energy for the reorientation of $[Fe(H_2O)_6]^{2+}$ is somewhat smaller than that of $[Ni(H_2O)_6]^{2+}$, whereas those for 180° flips of the water molecule for the two compounds agreed well. From our previous $^2H$ NMR studies of $[Co(H_2O)_6][SiF_6]$ and $[Mg(H_2O)_6][SiF_6]$, the activation energies for the reorientation of $[Co(H_2O)_6]^{2+}$ and $[Mg(H_2O)_6]^{2+}$ were determined as 82 and 62 kJ mol$^{-1}$, respectively [11, 12]. The values of the activation energy for the reorientation of $[M(H_2O)_6]^{2+}$

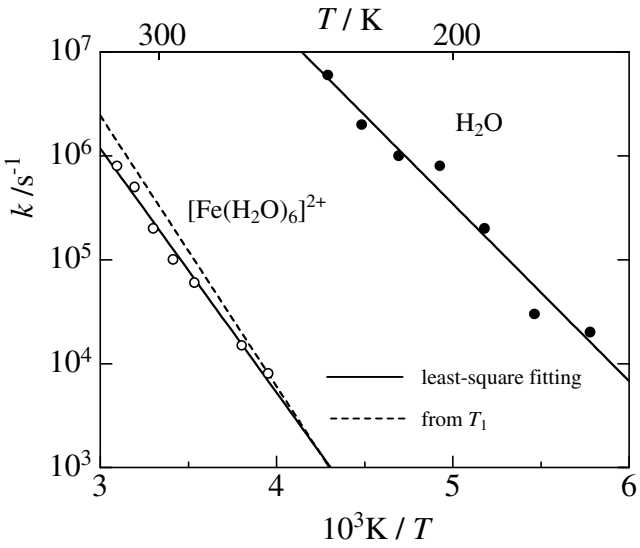


**Figure 9.** Temperature dependences of the jumping rates $k$ for the reorientation of $[Fe(H_2O)_6]^{2+}$ (○) and 180° flips of the water molecule (●) in $[Fe(H_2O)_6][SiF_6]$ estimated from $^2H$ NMR spectra. The solid lines show the results of the least-squares fitting. The broken line shows the result obtained from $T_1$.

increase in the order M: Fe < Mg < Co < Ni. For the activation energy of 180° flips of the water molecule, these four compounds have similar values. These results cannot be explained by the ionic radii of the metal ions. The local structure around $[M(H_2O)_6]^{2+}$ is predicted to affect the mobility of $[M(H_2O)_6]^{2+}$, since the activation energies of the $R\bar{3}m$-type compounds become smaller than those of the $R\bar{3}$-type compounds. The $[M(H_2O)_6]^{2+}$ octahedra in the $R\bar{3}m$-type compounds show a significant deformation, which is an elongation of the octahedron along the $C_3$ axis [1–7]. In contrast, the deformation of the octahedra is very weak in the $R\bar{3}$-type compounds. The elongated form is considered to cause a lowering of the activation energy for the reorientation about the $C_3$ axis.

## 4. Conclusions

The $^2H$ NMR spectrum of $[Fe(H_2O)_6][SiF_6]$ at high temperatures can be explained by six-site jumping of $[Fe(H_2O)_6]^{2+}$. The existence of this type of motion was also confirmed by the $^2H$ NMR $T_1$. These results suggest that the disorder of $[Fe(H_2O)_6]^{2+}$ in the high-temperature phase is dynamic. The activation energies of the reorientation of $[M(H_2O)_6]^{2+}$ in the $R\bar{3}m$-type compounds having disordered $[M(H_2O)_6]^{2+}$ were found to be smaller than those for the $R\bar{3}$-type compounds having ordered $[M(H_2O)_6]^{2+}$. For 180° flips of the water molecule, however, a large difference was rarely found in these compounds. A change in the crystal field of the $[Fe(H_2O)_6]^{2+}$ octahedron due to the phase transition was confirmed by the $^2H$ NMR $T_1$ and is considered to be correlated with the freezing of the reorientation of $[Fe(H_2O)_6]^{2+}$.

## References

[1] Hamilton W C 1962 *Acta Crystallogr.* **15** 353
[2] Chevrier G, Hardy A and Jéhanno G 1981 *Acta Crystallogr.* A **37** 578

[3] Ray S, Zalkin A and Templeton D H 1973 *Acta Crystallogr.* B **29** 2741
[4] Chevrier G and Saint-James R 1990 *Acta Crystallogr.* C **46** 186
[5] Ray S and Mostafa G 1996 *Z. Kristallogr.* **211** 368
[6] Chevrier G 1991 *Acta Crystallogr.* B **47** 224
[7] Chevrier G 1992 *J. Solid State Chem.* **99** 276
[8] Kassiba A, Hrabański R, Bonhomme D and Hader A 1995 *J. Phys.: Condens. Matter* **7** 3339
[9] Bose M, Roy K and Ghoshray A 1987 *Phys. Rev.* B **35** 6619
[10] Rager H 1981 *Z. Naturf.* a **36** 637
[11] Kimura J, Fukase T, Mizuno M and Suhara M 1998 *Z. Naturf.* a **53** 453
[12] Iijima T, Mizuno M and Suhara M 2000 *Z. Naturf.* a **55** 178
[13] Chiba T and Soda G 1968 *Bull. Chem. Soc. Japan* **41** 1524
[14] Iijima T, Orii K, Mizuno M and Suhara M 1998 *Z. Naturf.* a **53** 447
[15] Shiminovitch D J, Rance M, Jeffrey K R and Brown M F 1984 *J. Magn. Reson.* **58** 62
[16] Lin T-H, DiNatale J A and Vold R R 1994 *J. Am. Chem. Soc.* **116** 2133
[17] Vold R R 1994 *Nuclear Magnetic Resonance Probes of Molecular Dynamics* ed R Tycko (Dordrecht: Kluwer Academic)
[18] Greenfield M S, Ronemus A D, Vold R L, Vold R R, Ellis P D and Raidy T E 1987 *J. Magn. Reson.* **72** 89
[19] Barbara T M, Greenfield M S, Vold R L and Vold R R 1986 *J. Magn. Reson.* **69** 311
[20] Vold R R and Vold R L 1991 *Advances in Magnetic and Optical Resonance* vol 16, ed W S Warren (San Diego, CA: Academic)
[21] Rose M E 1957 *Elementary Theory of Angular Momentum* (New York: Wiley)
[22] Barnes R G 1974 *Advances in Nuclear Quadrupole Resonance* vol 1, ed J A S Smith (London: Heyden) p 335
[23] Birkland A and Svare I 1978 *Phys. Scr.* **18** 154
[24] Rubins R S, Clark J D and Jani S K 1977 *J. Chem. Phys.* **67** 893